

EXTRACTION OF ROAD JUNCTION ISLANDS FROM HIGH RESOLUTION AERIAL IMAGERY USING LEVEL SETS

M. Ravanbakhsh, C. Heipke, K. Pakzad

Institute für Photogrammetrie und GeoInformation, Leibniz Universität Hannover
Nienburger Str. 1, D-30167 Hannover, Germany -
(ravanbakhsh, heipke, pakzad) @ipi.uni-hannover.de

KEY WORDS: Road junction, Island, Level set, High resolution, Aerial image

ABSTRACT:

Road junctions are important components of a road network. However, they are usually not explicitly modelled in existing road extraction approaches. In this paper, we consider road junctions as area objects with possible existence of islands in their central area and propose a level set approach for the automatic extraction of islands. A region-based method is employed to initialize the level set function. The junction outline is provided to focus the attention on a specific area and some constraints are introduced to distinguish islands from other features such as cars. The approach was tested using aerial images of 0.1 m ground resolution taken from suburban and rural areas. Test results are presented and discussed in this paper.

1. INTRODUCTION

Geospatial databases contain various man-made objects among which roads are of special importance as they are used in a variety of applications such as car navigation. Road junctions are important components of a road network. However, they are usually not explicitly modelled in existing road extraction approaches. Road junctions in road network extraction systems have mainly been modelled as point objects at which three or more road segments meet (Gerke, 2006), (Zhang, 2003), (Barsi et al., 2002), (Wiedemann, 2002), (Hinz, 1999). In contrast, in (Gautama et al., 2004), (Mayer et al., 1998) and (Heipke et al., 1995) junctions are treated as planar objects. This kind of modelling does not always reflect the required degree of detail (Fig.1). A more detailed modelling of road junction is necessary for data acquisition in large scales.

In (Heipke et al., 1995), a strategy to extract roads in two different scales is proposed. In the fine resolution, roads are modelled as area objects and in coarse resolution as line objects. Results from both resolutions are merged using a rule based system. To delineate the junction area, segments next to accepted road segments are recursively investigated for homogeneity of the adjacent area. In (Gautama, 2004) a differential ridge detector in combination with a region growing operator is used to detect junctions and in (Mayer et al., 1998) a snake model is used to delineate junctions.



Figure 1. Superimposition of vector data on a high resolution aerial image

However, none of the described approaches tried to model small islands, which often are present in the central area of junctions. Since some junctions contain islands in their centre, a detailed junction model needs to consider the possible existence of small islands.

In this paper, we attempted to model islands. We use a level set approach for their automatic extraction. The junction outline is used as input to focus the attention on a limited area. Furthermore, some geometrical and topological constraints are defined to distinguish islands from other features. In section 2 the exploited level set formulation is illustrated. Various steps of the proposed strategy are described in section 3. In section 4, results from the implementation of the proposed approach using aerial gray level imagery of 0.1 m ground resolution are presented and evaluated. The paper concludes with a summary and an outlook.

2. LEVEL SET FORMULATION

A road junction can contain several small islands located in its central area. The number of islands varies in different junctions depending on the number of crossing roads and the junction's functionality. Islands are of diverse geometrical shape. Furthermore, they might be partially occluded by shadows from traffic lights, traffic signs and vehicles. These properties imply that the extraction of islands is a challenging problem in aerial image analysis. Furthermore, the number of islands in the junction is unknown. Therefore, it is crucial to be able to handle a change of topology of the curve that is to delineate islands. Geometric active contours provide a solution to the problem of the required change of topology.

Geometric active contours were introduced by (Caselles et al., 1993) and (Malladi et al., 1995) respectively. These models are based on curve evolution theory and level set methods. The basic idea is to represent contours as the zero level set of an implicit function in a higher dimension, usually referred to as

the level set function, and to evolve the level set function according to a partial differential equation (PDE). It was shown that a signed distance function ϕ , a function which introduces the minimum distance from every point in a defined domain Ω to the zero isocontour of a level set function, must satisfy the property of $|\nabla\phi|=1$ (Osher and Fedkiw, 2002). Therefore, the following formula is proposed

$$P(\phi) = \int_{\Omega} \frac{1}{2} (|\nabla\phi| - 1)^2 dx dy \quad (1)$$

as the internal energy term, which penalizes the deviation of ϕ from a signed distance function. Equations 1-12 were taken from the original paper (Li et al., 2005). $P(\phi)$ is a metric to characterize how close a function ϕ is to a signed distance function in $\Omega \subset R^2$. Along with the above defined functional $P(\phi)$, the following variational formulation is proposed

$$E(\phi) = \mu P(\phi) + E_m(\phi) \quad (2)$$

where $\mu > 0$ is a parameter controlling the effect of penalizing the derivation of ϕ from a signed distance function, and $E_m(\phi)$ is a certain energy that would drive the motion of the zero level curve of ϕ . Let I be an image, and g be the *edge indicator function* defined by

$$g = \frac{1}{1 + |\nabla G_\sigma * I|^2} \quad (3)$$

where G_σ is the Gaussian kernel with standard deviation σ . An external energy for a function $\phi(x, y)$ is defined by

$$E_{g,\lambda,v}(\phi) = \lambda L_g(\phi) + v A_g(\phi) \quad (4)$$

where $\lambda > 0$ and v is constant. $L_g(\phi)$ is a length term, and $A_g(\phi)$ is as an area term. They are defined by

$$L_g(\phi) = \int_{\Omega} g \delta(\phi) |\nabla\phi| dx dy \quad (5)$$

and

$$A_g(\phi) = \int_{\Omega} g H(-\phi) dx dy \quad (6)$$

respectively, where δ is the univariate Dirac function, and H is the Heaviside function (Osher and Fedkiw, 2002). The energy functional $L_g(\phi)$ in (5) computes the length of the zero level curve of ϕ . The energy functional $A_g(\phi)$ in (6) is introduced to speed up curve evolution as it decreases the area of the interior region $\Omega_\phi^- = \{(x, y) | \phi(x, y) < 0\}$ during the evolution. Note that, when the function g is constant ($g=1$), the energy functional in (6) is the area of the region Ω_ϕ^- . Now, the following total energy functional is defined

$$E(\phi) = \mu P(\phi) + E_{g,\lambda,v}(\phi) \quad (7)$$

The external energy $E_{g,\lambda,v}$ drives the zero level curve toward the object boundaries, while the internal energy $\mu P(\phi)$ penalizes the deviation of ϕ from a sign distance function during its evolution.

Using *calculus of variation* (Courant and Hilbert, 1953), the Gateaux derivative (first variation) of the functional E in (7) can be written as

$$\frac{\partial \phi}{\partial t} = -\mu[\Delta\phi - \text{div}(\frac{\nabla\phi}{|\nabla\phi|})] - \lambda\delta(\phi)\text{div}(g\frac{\nabla\phi}{|\nabla\phi|}) - vg\delta(\phi) \quad (8)$$

where Δ is the Laplacian operator. The function ϕ that minimizes this functional satisfies the Euler-Lagrange equation $\frac{\partial E}{\partial \phi} = 0$. The steepest descent process for minimization of the functional E is the following gradient flow:

$$\frac{\partial \phi}{\partial t} = \mu[\Delta\phi - \text{div}(\frac{\nabla\phi}{|\nabla\phi|})] + \lambda\delta(\phi)\text{div}(g\frac{\nabla\phi}{|\nabla\phi|}) + vg\delta(\phi) \quad (9)$$

This gradient flow is the evolution equation of the level set function used in our approach.

Since $\delta(\phi) = 0$ almost everywhere except for zero level curves, it seems unlikely that any standard numerical approximation will give a good approximation to the Eq. 5. Thus, in practice, the accurate smeared-out approximation of the Dirac function $\delta(x)$ is defined

$$\delta_\varepsilon(x) = \begin{cases} 0 & |x| > \varepsilon \\ \frac{1}{2\varepsilon} \left[1 + \cos\left(\frac{\pi x}{\varepsilon}\right) \right], & |x| \leq \varepsilon \end{cases} \quad (10)$$

where ε is a tunable parameter that determines the size of the bandwidth of numerical smearing. We used the regularized Dirac $\delta_\varepsilon(x)$ with $\varepsilon = 1.5$, for all the experiments in this paper, i.e. numerical computations are done within a stripe of three grid cells around the zero level curves. The approximation of (9) by the difference scheme can be simply written as

$$\frac{\phi_{i,j}^{k+1} - \phi_{i,j}^k}{\tau} = L(\phi_{i,j}^k) \quad (11)$$

where $L(\phi_{i,j})$ is the approximation of the right hand side in (9) by the spatial difference scheme. The difference equation (11) can be expressed as the following iteration:

$$\phi_{i,j}^{k+1} = \phi_{i,j}^k + \tau L(\phi_{i,j}^k) \quad (12)$$

It was found experimentally that the time step τ and the coefficient μ must satisfy $\tau\mu < \frac{1}{4}$, in order to maintain stable level set evolution. Using a larger time step can speed up the evolution, but may cause errors in the boundary location. The used variational level set formulation has two main advantages over the traditional level set formulations. First, a significantly larger time step can be used for numerically solving the

evolution partial differential equation, and therefore speeds up the curve evolution. Second, the need of costly re-initialization procedure is completely eliminated because the internal energy forces the level set function to be close to a sign distance function (Li et al., 2005).

3. EXTRACTION APPROACH

In this work, we make use of junction outlines obtained using an automatic approach for road junction extraction (Ravanbakhsh et al., 2007). This component together with the aerial imagery is regarded as input. Our strategy comprises three steps (Fig. 2). The obtained result consists of the extracted islands.

3.1 Segmentation

First, the junction outline where islands are located is clipped from the image. The search space for islands is further restricted to an area around the estimated junction centre point called *island area* with the size of $100 \times 100 \text{ m}^2$ (1000×1000 pixels) (Fig. 3-a). To begin the curve evolution, the initial level set function need to be constructed. It is computed within the island area. Segmentation as a necessary step can give a rough idea of

island regions from which the initial level set function is constructed. However, the segmentation results don't need to be topologically correct. We can also compute the initial level set function from a quadrilateral curve that encloses the islands. In such a case, however, the evolution needs high number of iterations to detect islands and many undesired features can be delineated as well. Using the segmentation results, the initial zero level curves are close to the solution. Therefore, with less number of iterations, islands can be detected. Furthermore, some undesirable features are discarded before the evolution begins. Thresholding is an appropriate method which is performed through gray value histogram analysis in order to segment islands assuming that the island area can be converted to a bimodal image area. The bimodal image area is provided by applying morphological operations. First, an opening operator is applied in order to remove distortions such as road markings (Fig. 3-b). Subsequently closing with the same structuring element is performed to eliminate small shadows etc. on islands (Fig. 3-c). Next, a Gaussian smoothing operator is applied followed by the thresholding operation (Fig. 3-d). At this stage, we consider convex areas inside the junction to be potentially islands, and the area surrounding them is built from asphalt.

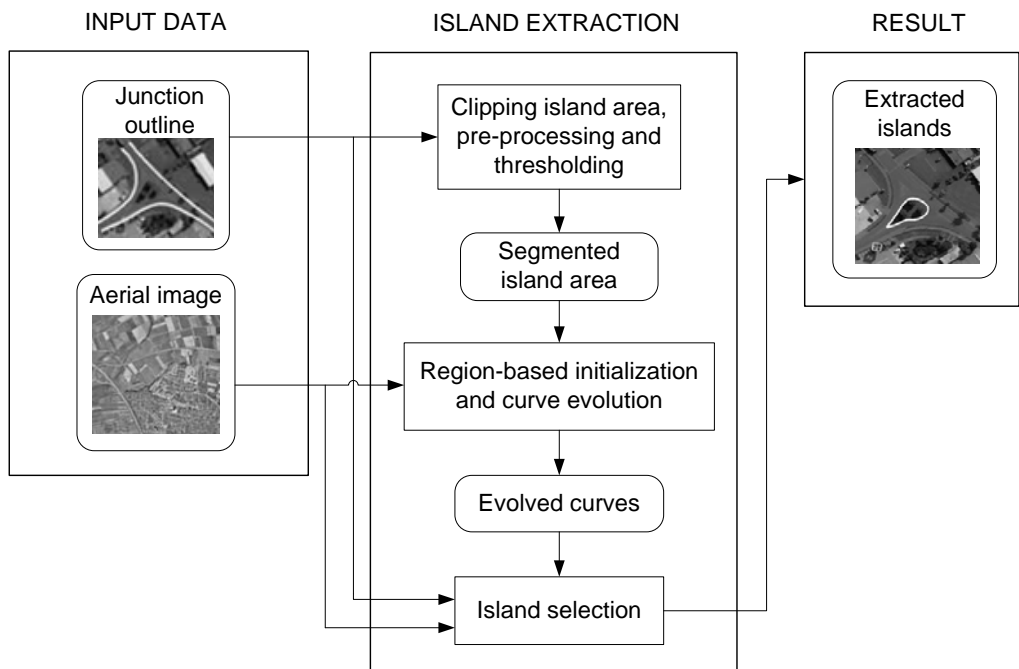


Figure 2. Proposed approach organisation

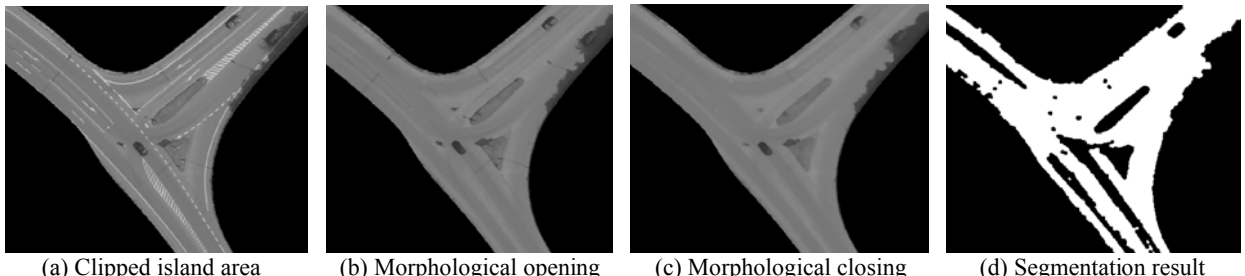


Figure 3. Illustration of the segmentation steps. In (b) and (c), a disk structuring element of size 5 is used for morphological operations. In (d), the threshold value is calculated to be 121 by gray value histogram analysis.

3.2 Initialization and curve evolution

The initial level set function is constructed from the segmented image so that areas in white are assigned a negative constant value and black areas take a positive constant value of the same magnitude. The zero level curves of the initial level set function is shown in Figure 4-b. They usually enclose the island border either entirely or in part, so they need to move toward the island boundaries. To achieve this goal, the coefficient of the weighted area term (v) in Equation 4 needs to be positive if the island surface is brighter than the surrounding asphalt area, and negative otherwise.

A positive v means shrinkage evolution whereas a negative v implies the expansion. In both cases, the zero level curves move toward islands. The question of whether the island surface is brighter or darker than its surrounding asphalt area can be answered by analysing the gray value histogram of the clipped island area. Then, the initial level set function will evolves according to the evolution equation (9), with its zero level curve converged to the exact boundary of islands (Fig. 4-b, c).

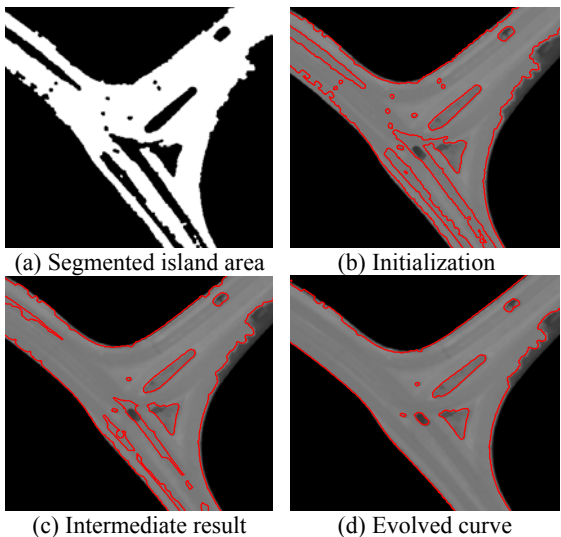


Figure 4. (a) The segmentation result, same as Fig. 3-d. (b) Zero level curves of the corresponding initial level set function. (c) Intermediate result of the zero level curve evolution with $\lambda=4$, $\mu=0.13$ and $v=-1.5$ (Iteration=50). (d) Zero level curves of the final level set function (Iteration=265).

3.3 Island selection

In order to select the curves converged to the island boundaries, some geometric and topological constraints are introduced based on the properties of islands, because, in addition to the islands, some undesirable features such as vehicles and large shadow areas might be extracted as island candidates (Fig. 5-a). Small closed areas such as cars are easily removed as their areas are below a certain threshold (Fig. 5-b).

Since island candidates must be located within the junction outline, those curves that lie on the junction outline are removed (Fig. 6). Furthermore, islands possess boundaries with a small curvature variation, so the contours with high curvature variations are eliminated (Fig. 7). Each curve needs to be approximated first to become smooth using cubic spline technique so that the slight variation of curvature values caused by small disturbances is avoided.

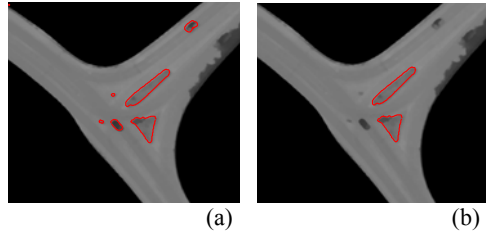


Figure 5. (a) Closed curves are retained as island candidates. (b) Two cars having areas 13 and 11 m^2 are eliminated. The remaining islands have areas 67 and 52 m^2 .

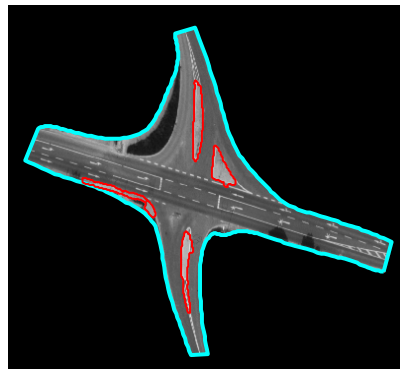


Figure 6. Illustration of the topological constraint. One of the obtained contours (left side) at some parts is located on the junction outline.

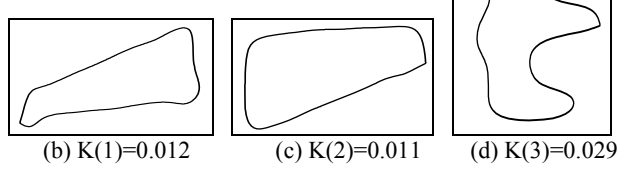
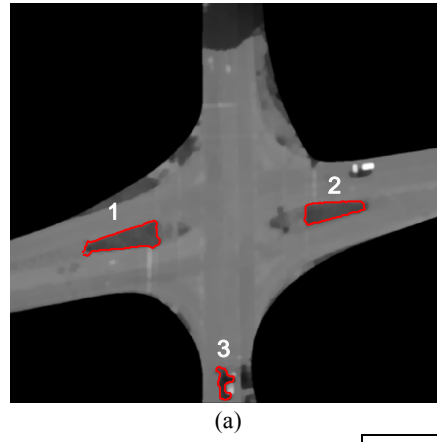


Figure 7. Illustration of the curvature constraint. (a) Islands labelled with numbers before applying curvature constraint. (b), (c) and (d) display the approximated curves 1, 2 and 3 and their computed mean curvature. The closed curve in (d) equals to area 3 is not considered as an island as its mean curvature value is too high.

4. RESULTS AND EVALUATION

We tested the proposed approach on a set of road junction samples with an identical set of control parameters for all samples. Some examples of results are given to show the capabilities of the new approach (Fig. 8). As can be seen, many islands were recovered. However, the bottom island in Figure 8-c cannot be extracted because the width of the island is too narrow. This problem can be observed in some other samples too (Fig 8-a, e). However, in these samples, except for a very small part, the whole island has been captured successfully. The reason why such a problem occurs is that the morphological operations cause the size of the island to decrease. As a result, the narrow parts of the islands are almost washed out. Another problem is poor contrast between the island surface and the surrounding asphalt area in which case the island is obliterated after pre-processing (Fig. 9-b) and consequently the island cannot be extracted.

In order to evaluate the performance of the approach, we compared the extracted islands to the manually digitized islands used as reference data. We selected 9 road junction samples that include 17 islands. The comparison is carried out by matching the extracted islands to the reference data using the so-called “buffer method” (Heipke et al., 1998). The buffer width can be defined according the required extraction accuracy for a specific application. We decided to set its value to 0.5 m in order to evaluate our method for the applications that require a high accuracy such as car navigation. An extracted island is assumed to be correct if the maximum distance between the extracted island border and its corresponding reference does not exceed the buffer width. Furthermore, a reference island border is assumed to be matched if whose maximum deviation from the extracted island border is within the buffer width. Based on these assumptions following quality measures used in our work are proposed:

- Completeness: is the ratio of the number of matched reference islands to the number of extracted islands

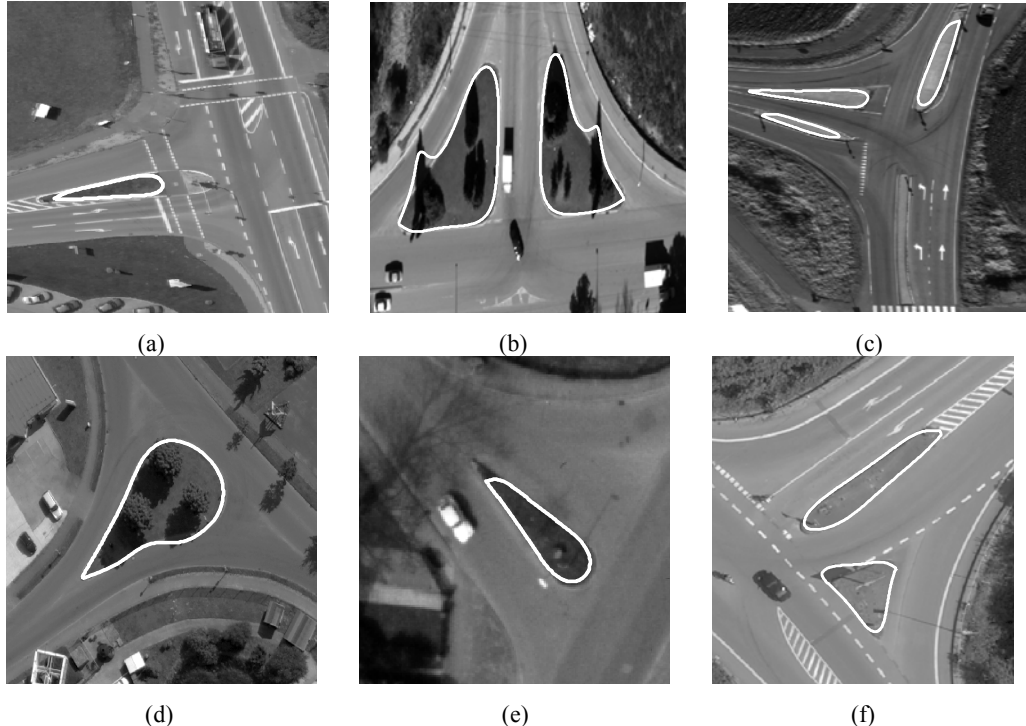


Figure 8. Results of the island extraction in various samples

- Correctness: is the ratio of the number of correctly extracted islands to the number of extracted islands
- Geometrical accuracy: is the average distance between the correctly extracted island and the corresponding reference island, which is expressed as Root Mean Square (RMS) value

Table 1 shows the evaluation result for the buffer width of 0.5 meter.

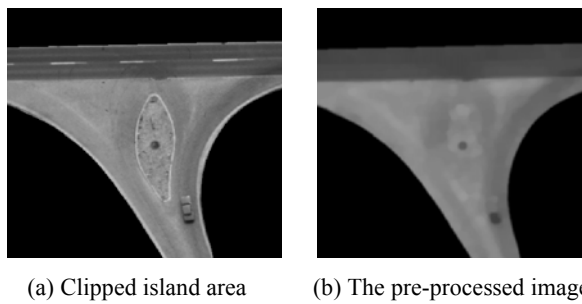
Reference number	Completeness	Correctness	Geometrical accuracy (m)
17	71 %	87 %	0.22

Table 1: Evaluation results

In one of samples (Fig. 10), tree shadows beside the border cause the extraction result to be out of the buffer area. Therefore, it cannot be considered as a correct result.

5. SUMMARY AND OUTLOOK

In this paper, we have proposed a new approach for the automatic extraction of small islands often appearing in the central area of junctions, which is based on a level set formulation. Furthermore, the initial level set function is constructed from the result of a segmentation procedure. The use of geometrical and topological constraints proved to be useful to distinguish islands from other undesirable detected features such as cars. Investigations into the integration of the island shape information and the internal energy of the level set formulation in order to overcome tree shadows are desirable. Our next goal will be the extraction of large central islands in roundabouts.



(a) Clipped island area (b) The pre-processed image

Figure 9. Failure result due to poor contrast

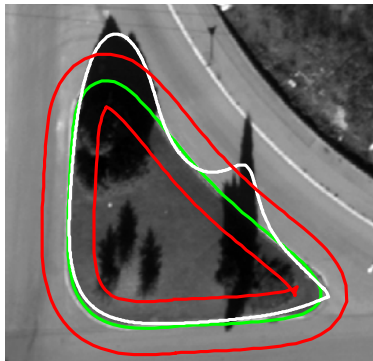


Figure 10. Shows a stripe with the buffer width of 0.5 m around the reference vector data (green). The white line exhibits the extraction result.

REFERENCES

- Barsi, A., Heipke, C., Willrich, F., 2002. Junction Extraction by Artificial Neural Network System – JEANS. In: *International Archives of Photogrammetry and Remote Sensing*, Vol. 34, Part 3B, pp. 18-21.
- Caselles, V., Catte, F., Coll, T., Dibos, F., 1993. A geometric model for active contours in image processing. In: *Numer.Math.*, vol. 66, pp. 1-31.
- Courant, R., Hilbert, D., 1953. *Methods of Mathematical Physics*. Wiley-Interscience, New York.
- Gautama, S., Goeman, W., D'Haeyer, J., 2004. Robust detection of road junctions in VHR images using an improved ridge detector. In: *International Archives of Photogrammetry and Remote Sensing*, Vol. XXXV, Part B3, Istanbul, pp. 815-819.
- Gerke, M., 2006. Automatic Quality Assessment of Road Databases Using Remotely Sensed Imagery. *Wissenschaftliche Arbeiten der Fachrichtung Geodäsie und Geoinformatik der Universität Hannover*, No. 261; also in: Deutsche Geodätische Kommission, Reihe C, No. 599.
- Heipke, C., Mayer, H., Wiedemann, C., Jamet, O., 1998. External evaluation of automatically extracted road axes, PFG 2, pp. 81-94.
- Heipke, C., Steger, C., Multhammer, R., 1995. A hierarchical approach to automatic road extraction from aerial imagery. In: McKeown, D.M., Dowman, I., (Eds.), *Integrating Photogrammetric Techniques with Scene Analysis and Machine Vision II*, SPIE Proceedings (2486), pp. 222-231.
- Hinz, S., Baumgartner, A., Steger, C., Mayer, H., Eckstein, W., Ebner, H., Radig, B., 1999. Road extraction in rural and urban areas. In: *Semantic Modeling for the Acquisition of Topographic Information from Images and Maps*. In: *SMATI'99*. München, pp. 7-27.
- Li, H., Xu, C., Gui, C., Fox, M.D., 2005. Level Set Evolution without Re-initialization: A New Variational Formulation. In: *Proceedings of IEEE conference on Computer Vision and Pattern Recognition (CVPR)*, IEEE Computer Society Press., pp. 430-436.
- Malladi, R., Sethian, J. A., Vemuri, B. C., 1995. Shape modeling with front propagation: a level set approach. In: *IEEE Trans. Patt. Anal. Mach. Intell.*, vol. 17, pp. 158-175.
- Mayer, H., Laptev, I., Baumgartner, A., 1998. Multi-Scale and Snakes for Automatic Road Extraction. In: *Proceedings of Fifth European Conference on Computer Vision*, Freiburg, Germany, Vol. 1406 of Springer Verlag Lecture Notes in Computer Science, pp. 720-733.
- Osher, S., Fedkiw, R., 2002. *Level Set Methods and Dynamic Implicit Surfaces*. Springer-Verlag, New York.
- Ravanbakhsh, M., Heipke C., Pakzad K., 2007. Road Junction Extraction from High Resolution Aerial Images. In: *International Archives of Photogrammetry and Remote Sensing*, Vol. XXXVI, Part 3 / W49B, Munich, pp. 131-138.
- Wiedemann, C., 2002. Improvement of Road Crossing Extraction and External Evaluation of the Extraction Results. In: *International Archives of Photogrammetry and Remote Sensing*, Vol. 34, Part 3B, pp. 297-300.
- Zhang, C., 2003. Updating of Cartographic Road Databases by Images Analysis. Ph.D. thesis, Institute of Geodesy and Photogrammetry, ETH Zurich, Switzerland, IGP Mitteilungen No. 79.